Electrostatics of a DNA-like Polyelectrolyte: Effects of Solvent Dielectric Saturation and Polarization of Ion Hydration Shells

Sergei Gavryushov*,† and Piotr Zielenkiewicz‡

Institute of Biocybernetics & Biomedical Engineering, Polish Academy of Science, Trojdena 4, 02-109 Warszawa, Poland, and Institute of Biochemistry and Biophysics, Polish Academy of Science, Pawinskiego 5a, 02-106 Warszawa, Poland

Received: July 20, 1998; In Final Form: November 18, 1998

The modified Poisson−Boltzmann (MPB) equations together with the Booth's theory of water dielectric saturation and an experimental dependence of water dielectric constant on ionic concentrations have been numerically solved to calculate the mean electrostatic potential and ionic distributions around a DNA-like highly charged cylindrical polyion. The model is explored for diluted mono- and multivalent electrolyte solutions. As follows from comparisons with the MPB and Poisson−Boltzmann (PB) calculations for the uniform permittivity solvent model, the solvent dielectric saturation and ion hydration shell polarization can be a significant contributor in the mean electrostatic potential and free energy of a highly charged macromolecule. Such effects may not be neglected in the case of a multivalent electrolyte. In contrast, the influence of solvent dielectric saturation and ionic polarization is negligible for a moderately charged spherical macroion, which confirms the success of numerous PB applications to calculations of p*K* values of protein charged groups.

Introduction

For the past 20 years the electrostatics of DNA has been a subject of continual interest because of strongly exhibited polyelectrolyte properties of DNA in solution. Although attempts to apply MD simulations to a model of DNA with ions have been recently reported,[1−5] they are computationally quite demanding. As a result, Monte Carlo (MC) simulations[1,6,7] and PB calculations [8,9] based on the continuum solvent model (the McMillan−Mayer level) remain practically applicable. Despite successful attempts to apply the PB equation to the evaluation of p*K* values of protein charged groups,[10−16] it is known that for multivalent electrolytes the equation can produce large errors even at low ionic concentrations. The last follows from comparisons of PB calculations with MC simulations[17−22] made for simplest geometry models of the electrical double layers. The PB equation is the simplest form of the double-layer statistical mechanical theory[17] and ignores the finite size of ions, interionic spatial correlations and polarization forces acting on an ion in nonuniform dielectric ("ion-image interactions"). The first two ones are responsible for the effect of "electrolyte overneutralization" or charge reversal observed in MC simulations with multivalent[17,22] and with concentrated monovalent[17,23] solutions. The ion-image forces take part in such phenomena as the increase in surface tension of electrolyte solutions[17] and salting-out of proteins.[24]

More advanced theoretical approaches within the framework of the continuum solvent model with finite size ions include the hypernetted-chain (HNC) integral equations,[25−27] the potential of mean force (PMF) approach[28] and the modified Poisson−Boltzmann (MPB) theory. Starting from works by Bell and Levine,[29−31] the last theory has been shown to be one of the most successful statistical mechanical theories of the electrical double layer.[17] The MPB theory has been gradually developed by Outhwaite and Bhuiyan who formulated the MPB equations for planar,[32] spherical,[33] and cylindrical[34] geometries within the framework of the restricted primitive model (RPM) of electrolyte. The last means that both anions and cations are treated as charged hard spheres imbedded in a dielectric continuum described by the dielectric constant.[17] Comparisons of MPB results with MC simulations for plane,[17] cylindrical[21,22] and spherical[20] double layers have shown that the MPB theory correctly describes the mean electrostatic potential and ionic distributions for relatively high concentrations of electrolyte and multivalent ions, where the PB equation fails qualitatively. The MPB theory is based on the Kirkwood hierarchy of equations together with the linearized Loeb's closure.[17] The theory was also formulated for the Bogoliubov−Born−Green−Yvon (BBGY) hierarchy of equations together with the same closure. This approach was initially studied by Outhwaite in the case of the plane geometry.[35] Higher-order closures[36] as well as an extension of the MPB theory to the three-component systems with solvent molecules[37,38] have been also studied. All applications of the MPB equations described above have been made for approximated solutions of the electrostatic boundary value problems for the fluctuation potential involved into the theory, which can be done only for simplest geometries. The numerical implementation of the three-dimensional (3D) MPB equations together with linearized Loeb's closure has been reported in works by Gavryushov and Zielenkiewicz,[39−41] which allows the MPB equations to be applied to an arbitrary geometry electrostatic double layer, i.e., to the all-atom model of a macromolecule.[40,41]

One of important features of the MPB equations is that they incorporate the ion-image forces in a more natural way than any current theory of the electrical double layer. It allows a

* Corresponding author. Tel.: +48 22 6597030 (207). Fax: +48 22 6597030. E-mail: sergei@ibib.waw.pl.
† IBBE.
‡ IBB.

10.1021/jp983081i CCC: $18.00
Published on Web 06/25/1999

possible influence of solvent dielectric saturation and polatization of ion hydration shell on the electrostatic potential and ionic distributions to be studied. These effects were approximately incorporated into the initial formulation of the MPB theory by Bell and Levine,[29−31] but only the uniform permittivity solvent model was explored in later works.

The effects of dielectric saturation of the solution on properties of electrolytes and electrical double layers have been a subject of discussion through many decades. It is usually assumed that such effects are weak. Many years ago, using an experimental dependence of water permittivity on ionic concentration, Levine showed that for not-too-highly charged double layers and at low concentrations of ions these effects may be considered as negligible.[30] Recently evidence of notable dielectric saturation of water in the vicinity of DNA has appeared.[42−45] As follows from measurements and MD simulations, the local dielectric constant of water in the minor groove of DNA appears to be in the range of 20−30 instead of about 80 for pure water. This result was confirmed in a work by Lamm and Pack[46] where the authors combined the Booth's theory of dielectric saturation[47] and the dependence of permittivity on ionic concentration with the PB equation. It is important to note that this method may lead to serious errors because of the mentioned above impossibility of the PB equation to describe polarization forces acting on an ion in a nonuniform dielectric. For example, the free energy of ionic solvation reaches hundreds kcal per mole, and this can be described in terms of continuum electrostatics (the Born model).[48] On the other hand, an application of the PB equation to ionic solvation leads to a zero mean force acting on ions close to the water−air interface due to obvious zeroing the mean electrostatic potential in the case of a symmetrical electrolyte. In contrast, the MPB theory correctly describes the Born energy of ion hydration (see below).

In the present work the MPB equations based on the Kirkwood hierarchy, the Booth's theory of water dielectric saturation, and experimental dependence of water dielectric constant on ionic concentrations are combined to study the ionic distributions and mean electrostatic potential near a highly charged cylinder representing a simplified model of DNA. The model is explored only for diluted 1:1 and 2:1 electrolytes. This approach is also applied to calculations of the free energy of a charged spherical macroion in electrolyte solution to see an influence of dielectric saturation on the thermodynamics of a macromolecule.

Theory

The Booth's theory of dielectric saturation gives the following expression for the dielectric constant of water in the presence of high electric field strength (E):[46,47]

$$\epsilon = n^2 + (\epsilon_0 - n^2)L(x) \tag{1}$$

where ϵ_0 is the bulk dielectric constant, $x = \sqrt{73(n^2+2)}\mu_0 E/6kT$, n is the optical refractive index of water, μ_0 is the dipole moment of the water molecule, $L(x)$ is a Langevin-type function $3[\coth(x) - 1/x]/x$.

To evaluate forces acting on an ion in a nonuniform dielectric, one has to define the structure of a low dielectric constant cavity representing the hydrated ion in water. Recently such a cavity model has been successfully used in predictions of measured solvation free energies for small molecules[49,50] as well as in attempts to validate the Born radius of ionic hydration using HNC calculations,[51,52] MC,[53,54] and MD[55,49] simulations. The radius of the dielectric cavity can be treated not only as a parameter to fit data of the ionic solvation, but also in terms of a water dielectric constant dependence on ionic concentration. At low ionic concentrations the dielectric decrement of water is given by[46,56,57]

$$\epsilon/\epsilon_0 = 1 - \frac{3}{2}\frac{\epsilon_0 - \epsilon_i}{\epsilon_0}\rho \tag{2}$$

where $\epsilon_i \sim 2$ is the dielectric constant within the cavity, that is the dielectric constant of a solvated ion-frozen water complex, ϵ_0 is the dielectric constant of bulk water and ρ is local volume fraction of ions. Experimentally measured dependences (2) for various ions were published in the literature.[58,57] The experimental relationship between the dielectric constant and the concentration of ions is

$$\epsilon = \epsilon_0 + \Sigma\delta_i c_i \tag{3}$$

where c_i is the concentration of ions of species i in moles per liter, δ is a negative constant. The electrolyte solutions were investigated up to the concentration of 2 M. Experimental values are $\delta_{Na^+} + \delta_{Cl^-} = -16$ for NaCl[57] and $\delta_{Mg^{2+}} + 2\delta_{Cl^-} = -30$ for $MgCl_2$.[58] Taking $\delta_{Na^+} = \delta_{Cl^-} = -8$ (as the simplest interpretation of the experimental data) or $\delta_{Mg^{2+}} = -24$ (as suggested in ref 58), one obtains the dielectric cavity radius of about 3 Å through eqs 2 and 3. The last result is in a reasonable agreement with the cavity radii about 2 Å from the Born model applied to hydration enthalpies of ions.[48]

The Kirkwood hierarchy together with linearized Loeb's closure gives the following equations for distributions of ions of species α, represented by hard spheres of diameter d:[29−31]

$$\ln g_\alpha(\mathbf{r}) = \ln \xi_\alpha(\mathbf{r}) - \beta q_\alpha \psi(\mathbf{r}) + \frac{\beta}{8\pi}(\nabla\psi)^2\left(\frac{\partial\epsilon}{\partial n_\alpha}\right)_{T,D} - \beta q_\alpha \int_0^1 d\lambda\{\eta_\alpha(\mathbf{r}|\lambda) - \eta_\alpha(\infty|\lambda)\} \tag{4}$$

where $\beta = 1/kT$, q_α is the charge of an ion, $\psi(\mathbf{r})$ is the mean electrostatic potential, and the mean ionic concentration $n_\alpha(\mathbf{r})$ is expressed via the ionic bulk concentration n_α^0 and the distribution function $g_\alpha(\mathbf{r})$ as $n_\alpha(\mathbf{r}) = n_\alpha^0 g_\alpha(\mathbf{r})$. The right-hand side of eq 4 is the potential of mean force (PMF), acting on the ion, divided by $-kT$. The first term of the PMF appears due to the work required to insert an uncharged ion at point $\mathbf{r}$ and denoted as $-kT \ln \xi_\alpha(\mathbf{r})$. The fourth term of the PMF is due to different ion's self-atmosphere energies at position $\mathbf{r}$ and at infinity, ion-image interactions, and the work of diffuse charge distribution removal from the spherical exclusion volume of ion. The third term on the right side of eq 4 was initially considered in works by Prigogine, Mazur and Defay,[59] Bolt,[60] Sparnaay,[61] and Levine[29−31] (see also ref 56). This is just the polarization energy of a dielectric cavity representing an ion in the external electric field (i.e. the polarization energy of the ion hydration shell) taken at constant temperature T and electrical displacement D. From experimental dependence (3), it may be assumed that $\partial\epsilon/\partial n_i = (10^3/N_A)\delta_i$ where n is expressed in cm^{-3}. The Kirkwood hierarchy yields the following equation for $\eta_\alpha(\mathbf{r}|\lambda)$:

$$\eta_\alpha(\mathbf{r}_2|\lambda) = \lim_{\mathbf{r}_1 \to \mathbf{r}_2}\left[\phi_\alpha(\mathbf{r}_1,\mathbf{r}_2|\lambda) - \frac{\lambda q_\alpha}{\epsilon_i r_{12}}\right] \tag{5}$$

where $q_\alpha/(\epsilon_i r_{12})$ is Coulombic self-potential of the point charge q_α in a medium of dielectric constant ϵ_i and $\phi_\alpha(\mathbf{r}_1,\mathbf{r}_2|\lambda)$ is the fluctuation potential. The last can be written as a sum of two terms: $\phi_\alpha(\mathbf{r}_1,\mathbf{r}_2|\lambda) = \phi^\rho(\mathbf{r}_1,\mathbf{r}_2) + \phi_\alpha{}^\delta(\mathbf{r}_1,\mathbf{r}_2|\lambda)$. The $\phi^\rho(\mathbf{r}_1,\mathbf{r}_2)$ term

is the potential due to the diffuse charge neutralization within the exclusion volume of the ion at point $\mathbf{r}_2$. The $\phi_\alpha{}^\delta(\mathbf{r}_1,\mathbf{r}_2|\lambda)$ term is the potential due to the fixed at $\mathbf{r}_2$ and gradually charged ion of species α, its Debye−Huckel atmosphere, and the polarization charges of the dielectric cavity of this ion. The fluctuation potential satisfies approximate equations for the hard sphere short-range interionic interactions and spherical dielectric cavity model of hydrated ions:

$$\nabla_1^2\phi_\alpha(\mathbf{r}_1,\mathbf{r}_2|\lambda) = 0 \tag{6.1}$$

(inside the macromolecule's interior and the shell of ionic exclusion around the macromolecule)

$$\nabla_1(\epsilon(\mathbf{r}_1)\nabla_1\phi^\rho(\mathbf{r}_1,\mathbf{r}_2)) = -\nabla_1(\epsilon(\mathbf{r}_1)\nabla_1\psi(\mathbf{r}_1)) \tag{6.2.1}$$

$$\nabla_1(\epsilon_\delta(\mathbf{r}_1,\mathbf{r}_2)\nabla_1\phi_\alpha^\delta(\mathbf{r}_1,\mathbf{r}_2|\lambda)) = -4\pi\lambda q_\alpha\delta(\mathbf{r}_1-\mathbf{r}_2) \tag{6.2.2}$$

(within the ionic atmosphere around the macromolecule, $r_{12} < d$)

$$\nabla_1(\epsilon(\mathbf{r}_1)\nabla_1\phi_\alpha(\mathbf{r}_1,\mathbf{r}_2|\lambda)) = k^2(\mathbf{r}_1)\phi_\alpha(\mathbf{r}_1,\mathbf{r}_2|\lambda) \tag{6.3}$$

(within the ionic atmosphere around the macromolecule, $r_{12} > d$)

where $\epsilon(\mathbf{r})$ is the dielectric constant of solvent dependent on ionic concentrations and electric field strength through eqs 1 and 3,

$$\epsilon_\delta(\mathbf{r},\mathbf{r}_2) = \begin{cases}\epsilon(\mathbf{r}), |\mathbf{r}-\mathbf{r}_2| > a_\epsilon \\ \epsilon_i, |\mathbf{r}-\mathbf{r}_2| < a_\epsilon\end{cases}$$

ϵ_i and a_ϵ are the internal dielectric constant and the radius of the dielectric cavity of the ion, respectively ($a_\epsilon < d$)

$$k^2(\mathbf{r}) = 4\pi\beta\sum_\gamma n_\gamma(\mathbf{r})q_\gamma^2$$

$$\epsilon(\mathbf{r}) = \epsilon_B(\mathbf{r}) + \Sigma\delta_i\, 10^3\, n_i(\mathbf{r})/N_A \tag{7}$$

ϵ_B is calculated through eq 1.

No boundary effects on the solvent-accessible surface[46] are evaluated for the calculation of $\epsilon(\mathbf{r})$. To avoid the problem, a relatively higher thickness of the ion exclusion zone (3 Å) is taken and all calculations for the cylindrical model of DNA are restrained to diluted electrolytes. The dielectric constant of solvent can be notably reduced within the ion exclusion zone around a macromolecule (the Stern layer).[62] In the present work this value is taken equal to the dielectric constant obtained on the ion-accessible surface via eq 7.

The mean electrostatic potential $\psi(\mathbf{r})$ from eq 4 satisfies the Poisson equation

$$\nabla^2\psi(\mathbf{r}) = -\frac{4\pi}{\epsilon_m}\rho_0(\mathbf{r}) \quad \text{inside the macromolecule,}$$

$$\nabla(\epsilon(\mathbf{r})\nabla\psi(\mathbf{r})) = -4\pi\sum_\gamma q_\gamma n_\gamma(\mathbf{r}) \quad \text{outside the macromolecule} \tag{8}$$

where ρ_0 is the charge density of the macromolecule and ϵ_m is its permittivity.

For both the fluctuation potential and $\psi(\mathbf{r})$, the boundary conditions require continuity in the potentials and its normal derivatives multiplied by the dielectric constant of the medium. At low ionic concentrations, the exclusion volume term $\ln \xi_\alpha(\mathbf{r}_2)$ may be approximated by[31] $-\int_{V_\alpha}\sum_\gamma(n_\gamma(\mathbf{r})-n_\gamma{}^0)d^3\mathbf{r}$, where $V_\alpha = 4/3\ \pi d^3$ is the excluded volume of an ion of diameter d centered at position $\mathbf{r}_2$. By neglecting the first, third, and fourth terms of the right part of eq 4 and substituting into eq 8 at $\epsilon(\mathbf{r}) \equiv \epsilon_0$, eq 8 becomes the PB equation. Its solution gives initial $\psi^{(0)}(\mathbf{r})$, which makes it possible to obtain $\phi_\alpha^{(0)}(\mathbf{r}_1,\mathbf{r}_2)$ through eq 6, then one obtains $g_\alpha^{(1)}(\mathbf{r})$ through eqs 5 and 4 and $\psi^{(1)}(\mathbf{r})$ through eq 8 and so on. This procedure was applied to models of DNA in a uniform permittivity solvent, where a very fast convergence of loop (8)−(6)−(4)−(8) was observed.[39, 41]

In the particular case of the infinitely long, charged cylinder representing DNA, eq 8 is reduced to the ordinary differential equation

$$\frac{1}{r}\frac{d}{dr}\left(r\epsilon(r)\frac{d}{dr}\psi(r)\right) = -4\pi\sum_\gamma q_\gamma n_\gamma(r) \tag{9}$$

subject to the two boundary conditions

$$\left.\frac{d\psi(r)}{dr}\right|_{r=R_C} = 0 \tag{10.1}$$

$$\left.\frac{d\psi(r)}{dr}\right|_{r=r_0} = -\frac{4\pi\sigma_0}{\epsilon(r_0)} \tag{10.2}$$

where r_0 is a radius of the cylinder together with the ion exclusion zone and R_C is the radius of the cell (the so-called cell model[21,22]), σ_0 is the surface charge density of the cylinder evaluated for the outer surface the ion exclusion zone. It should be noted that the thickness of the Stern layer may differ from the hydrated radius of an ion (i.e., the hard sphere radius in the RPM model).[40] Similarly, eq 8 can be written for a uniformly charged spherical macroion:

$$\frac{1}{r^2}\frac{d}{dr}\left(r^2\epsilon(r)\frac{d}{dr}\psi(r)\right) = -4\pi\sum_\gamma q_\gamma n_\gamma(r) \tag{11}$$

together with boundary conditions (10).

The derivation of eqs 4−8 is based on three assumptions in addition to the hard sphere model of the ion−ion short range interactions. One is that solvent polarization effects created by an ion are reduced to the Born dielectric cavity model. The second assumption is that the distribution function of solvent molecules may be ignored, i.e., the determination of $\epsilon(\mathbf{r})$ via eqs 1 and 7 is based on the uniform density solvent approximation. The third assumption is that the ion hydration shell of water molecules is not affected by the mean electric field. The substitution of the experimental dependence $\epsilon(C_{ions})$ (eq 3) in the third term of the PMF (eq 4) is based on this assumption. A justification of these assumptions is discussed below, in Results and Discussion. It is important to note that eqs 4−8 are quite exact within the framework of this model.

One can see from eqs 6.2 and definition of ϵ_δ that the Born expression of ion solvation energy is explicitly described by the MPB eqs 4−8. For a single ion in solvent, $\phi^\rho \equiv 0$ and ϕ^δ is just the electrostatic potential of a point-like ion charge λq_α centered at the low dielectric constant spherical cavity at point $\mathbf{r}_2$. Then $\eta_\alpha(\mathbf{r}_2|\lambda)$ is the electrostatic potential of all polarization charges surrounding the point charge λq_α and $q_\alpha\int_0^1 d\lambda\eta_\alpha(\mathbf{r}_2|\lambda)$ yields the corresponding polarization energy of ion charging. For the uniform dielectric of permittivity ϵ it is just $(q^2\alpha/2a_\epsilon)(1/\epsilon - 1/\epsilon_i)$. Then the PMF difference at a transfer of

the ion from air ($\epsilon = 1$) into water ($\epsilon = \epsilon_0$) is $(q^2_\alpha/2a_\epsilon)(1/\epsilon_0 - 1)$, i.e., the Born formula of solvation energy.

The electrostatic part of the macromolecule's chemical potential can be obtained via two processes: a transfer of the uncharged macromolecule into electrolyte solution and charging up the macromolecule:[40]

$$W = W_0 + W_{Ch} \tag{12}$$

For a sufficiently dilute macromolecular solution,

$$W_{Ch} = \int_0^1 d\xi \int d^3\mathbf{r}\rho_0(\mathbf{r})\psi(\mathbf{r},\xi) \tag{13}$$

where $\psi(\mathbf{r},\xi)$ is a solution of eqs 4−8 at charge density of the macromolecule equal to $\xi\rho_0(\mathbf{r})$. At low ionic concentrations

$$W_0 = kT\sum_\gamma \int (n^0_\gamma - n_\gamma(\mathbf{r}))d^3\mathbf{r}$$

The more exact expression of W_0 is

$$W_0 = \sum_\gamma n^0_\gamma \left(kT - \frac{q^2_\gamma K}{4\epsilon_0(1+Kd)^2}\right) \int (1-g_\gamma(\mathbf{r}))d^3\mathbf{r} \tag{14}$$

(see Appendix 1), where $g_\gamma(\mathbf{r})$ are obtained from eqs 4−8 at $\rho_0 = 0$ and K is the inverse Debye−Huckel length for bulk electrolyte.

Method. The method of the finite-difference (FD) numerical solution of a system of equations similar to eqs 4−8 has been described in refs 39−41. A new important feature of eq 6.2.2 is the relatively small spherical cavity of a low dielectric constant medium surrounding the point charge at point $\mathbf{r}_2$. This requires a shorter grid spacing in the vicinity of the singularity position $\mathbf{r}_2$ as the spacing should be much lower than the diameter of the dielectric cavity. As a result, a several steps focusing technique of the fluctuation potential FD calculations has been applied to the numerical solution of eq 6 just as it is widely used for the solutions of the PB equation.[63] The FD grid is always centered at the δ function position. The highest grid resolution corresponds to 15−20 grid nodes per the diameter of the dielectric cavity $2a_\epsilon$, i.e., about 3 grid/Å. The initial size of the grid corresponds to the doubled sum of ionic exclusion radius d (4 Å) and 5−6 Debye−Huckel lengths λ_{DH} for bulk electrolyte. At ionic strength of 0.05 M ($\lambda_{DH} \sim 13$ Å) and 61 × 61 × 61 point lattice, it leads to the initial grid spacing of about 2 Å.

Assigning the δ function position to the lattice node, the η function is evaluated as[41]

$$\int_0^1 d\lambda\{\eta_\alpha(\mathbf{r}|\lambda) - \eta_\alpha(\infty|\lambda)\} \approx \frac{1}{2}[\phi^\delta_\alpha(\mathbf{r},\mathbf{r}|1) - \phi^\delta_\alpha(\infty|1)] + (\phi^\rho(\mathbf{r},\mathbf{r}) - \phi^\rho(\infty)) \tag{15}$$

In both cases of the charged cylinder and the charged sphere considered in the present work, the function $n\nu(r)$ from eqs 9 and 11 is written as

$$n_\nu(r) = n^0_\nu \xi_\nu(r) \exp(-\beta q_\nu \psi(r) - \beta U^{pol}_\nu(r) - \beta U^{csi}_\nu(r)) \tag{16}$$

where

$$U^{pol}_\nu(r) = -\frac{1}{8\pi}\left(\frac{d\psi(r)}{dr}\right)^2 \frac{\partial\epsilon}{\partial n_\nu}$$

is the polarization term and

$$U^{csi}_\nu(r) = q_\nu \int_0^1 d\lambda\{\eta_\nu(\mathbf{r}|\lambda) - \eta_\nu(\infty|\lambda)\}$$

is the term due to the interionic correlations, finite size of ions, and ion−image electrostatic interactions. The functions $\xi_\nu(r)$, $U^{pol}{}_\nu(r)$ and $U^{csi}{}_\nu(r)$ result from FD solutions of 3D eqs 6 for about 30 points $\mathbf{r}_2$ lying on the radial line outside the cylinder (sphere). The distance between neighboring points is taken as the initial grid spacing for focusing calculations. Calculated discrete values of $\xi_\nu(r)$, $U^{csi}_\nu(r)$, and $U^{pol}_\nu(r)$, are interpolated by cubic splines.

Testing. The algorithm described above has been intensively tested as it differs from the algorithm described in refs 39−41. A comparison of numerically calculated electrostatic energy differences with theoretical values for a point charge centered in a small dielectric cavity (the Born energy) has shown a good accuracy at grid spacings and cavity diameters described in the previous section. To test the focusing technique algorithm, ionic distributions and electrostatic potentials have been obtained for a model of the 8 Å radius highly charged cylinder at surface charge density equal to that of DNA. The solvent was represented by a uniform dielectric medium of permittivity set to 80, ion diameter d was set to 4 Å; the diameter $2a_\epsilon$ of a dielectric cavity of the ion was taken as 6 Å. The cavity dielectric constant ϵ_i is 2. This model of 2:1 electrolyte have been explored at two salt concentrations: $C_{2:1} = 0.017$ M ($\lambda_{DH} = 13.6$ Å) and $C_{2:1} = 0.167$ M ($\lambda_{DH} = 4.3$ Å). In both cases there was an excellent agreement between the results for the cavity model of ion (the focusing technique of fluctuation potential calculations) and for the point-charge model applied in ref 39. In the last case, the charge of the ion is imbedded into a uniform permittivity solvent and no focusing is used, which results in computationally more expensive FD grids (101 × 101 × 101 nodes). The differences in electrostatic potentials and ionic distributions obtained in the two methods are within a couple percent.

Results and Discussion

MPB calculations of the mean electrostatic potential and ionic distributions have been carried out for a cylindrical polyion placed into diluted solutions of 1:1 and 2:1 electrolytes. The Booth's theory of dielectric saturation (eq 1) together with the decrease of water dielectric constant due to the presence of ions (eq 7) predicts strong saturation effects in the vicinity of the cylinder.[46] It may cause a significant additional repulsion of counterions from the polyion since the magnitude of the ion self-energy is very high and strongly dependent on the local dielectric constant. This repulsion decreases the local ionic concentrations near the surface of the polyion. A result is the lower screening of the electric field of the polyion, which, in return, may lead to more pronounced dielectric saturation of the surrounding solution and a higher additional repulsion of counterions in the vicinity of the macromolecule. It should lead to an increase of the "effective radius" of the polyion in terms of ionic distributions and, finally, to higher electrostatic energy of the macromolecule.

The described picture is clearly seen from Figure 1, where ionic distributions around a highly charged cylinder are calculated through eqs 4−9 together with eq 1 for 0.05 M 1:1 electrolyte ($\lambda_{DH} = 13.6$ Å). The model is an 8 Å radius cylinder having the surface charge density equal to that of the DNA (this corresponds to negative charges placed apart on the axis of the cylinder with 1.7 Å displacement). The thickness of the Stern layer of ionic exclusion is taken as 3 Å, which yields $r_0 = 11$

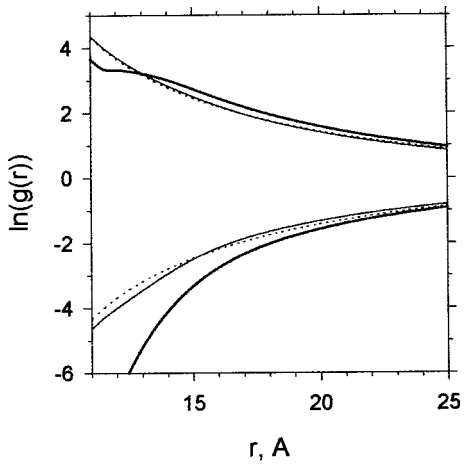

Figure 1. Ion distributions around DNA-like cylindrical polyion for 1:1 electrolyte. The thick solid lines are MPB results for the solvent dielectric saturation model; the thin solid lines are MPB results for the RPM; the dotted lines correspond to the solution of the PB equation.

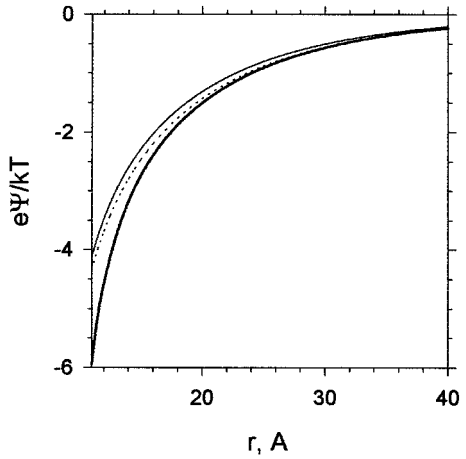

Figure 2. Mean electrostatic potentials corresponding to data shown in Figure 1. Notation as in Figure 1; e is the proton charge.

Å (eq 10.2); $d = 4$ Å; $n = 1.33$; $\mu_0 = 2.1$ D (eq 1);[47] $2a_\epsilon = 6$ Å; $\epsilon_i = 2$; the dielectric constant of pure water ϵ_0 from eq 1 is set to 78.5; the dielectric constant ϵ_m of the interior of the cylinder is taken as 2; the ion hydration shell polarization parameters $\delta_{anion} = \delta_{cation} = -7.5$. This set of solvent and ion parameters is applied to other calculations described below, except for constants a_ϵ and δ in the case of divalent ions. The $61 \times 61 \times 61$ nodes grid was used to solve eq 6. The corresponding grid spacing was 1.94 Å for the initial FD calculations of the fluctuation potential terms ϕ^δ and ϕ^ρ. For the first and second focusing calculations, the grid spacing was 0.96 and 0.48 Å, respectively. The parameter R_C from eq 10.1 was set to 125 Å, i.e., about $8.4\lambda_{DH}$ away from the cylinder. In other words, the polyion at infinity dilution is considered.

Results of corresponding MPB calculations for the RPM electrolyte are also shown in Figure 1. One can see that despite a good agreement between MPB and PB results in the case of solvent uniform permittivity, there is a difference between these results and curves obtained for the solvent dielectric saturation model. The additional repulsion of both co- and counterions is reflected in a shift of the ion distribution curves away from the cylinder and, more importantly, in an increase of the absolute magnitude of the mean electrostatic potential on the ion-accessible surface (Figure 2). The last effect increases the electrostatic part of the free energy of the polyion since the additional repulsion of ions is the positive work against the mean

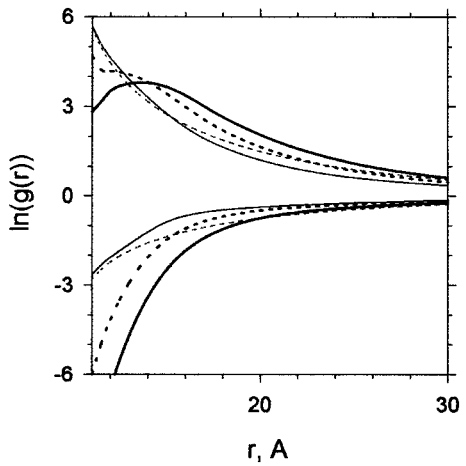

Figure 3. Ion distributions around DNA-like cylindrical polyion for 2:1 electrolyte. Notation as in Figure 1. The thick solid line corresponds to the model with highly polarizable divalent counterions ($\delta_{2+} = -24$). The thick dotted line corresponds to results at $\delta_{2+} = -7.5$.

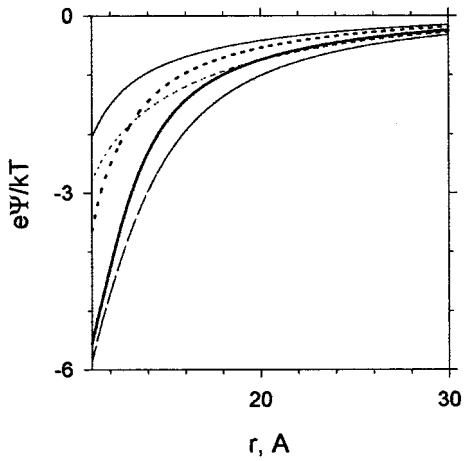

Figure 4. Mean electrostatic potentials corresponding to data shown in Figure 3. Notation as in Figure 3. The thin dashed line is the potential obtained at $2a_\epsilon = 4$ Å instead of $2a_\epsilon = 6$ Å.

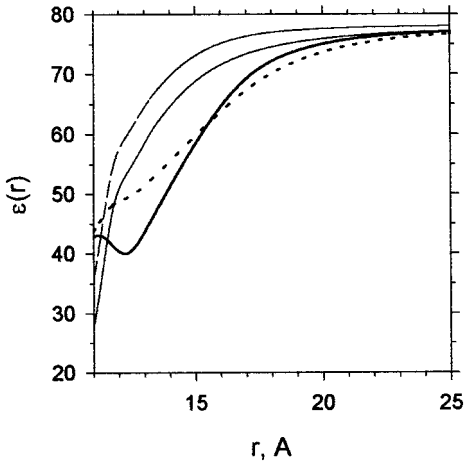

Figure 5. Local dielectric constant in models corresponding to Figures 1−4. The thin solid line corresponds to $\epsilon(r)$ for 1:1 electrolyte. The dashed line is $\epsilon(r)$ for 2:1 electrolyte, $\delta_{2+} = -7.5$, $2a_\epsilon = 6$ Å. The thick solid and dotted lines are $\epsilon(r)$ functions for 2:1, $\delta_{2+} = -24$ electrolyte at $2a_\epsilon = 6$ Å and $2a_\epsilon = 4$ Å, respectively.

electric field and osmotic pressure of the ionic gas. The resulting drop of the local dielectric constant $\epsilon(r)$ is shown in Figure 5.

The effects described above are more strongly exhibited in the case of 0.017 M 2:1 electrolyte (the ionic strength and the

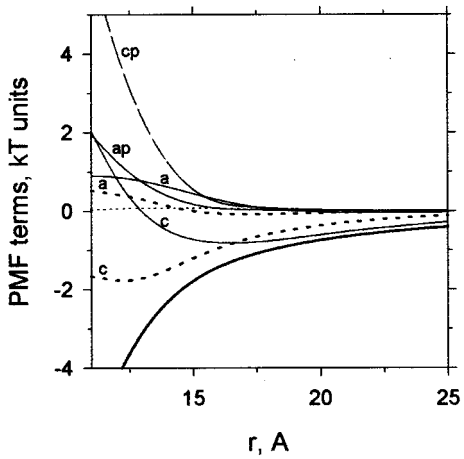

Figure 6. PMF terms for the model corresponding to Figures 3 and 4, 2:1 electrolyte. $\delta_{2+} = -24$. The thin solid lines are $U^{csi}(r)$ functions of anions (co-ions) and cations (counterions) for the solvent dielectric saturation model. The dashed lines labeled "ap" and "cp" correspond to $U^{pol}(r)$ functions for anions and cations, respectively. The thin dotted line is the volume exclusion term $-kT \ln \xi(\mathbf{r})$ of the PMF. The thick dotted lines are $U^{csi}(r)$ functions for the RPM. The thick solid line is the $e\psi(r)$ term.

λ_{DH} are equal to those of the 1:1 electrolyte model). In Figure 3 the MPB ionic distributions of divalent counterions (cations) and monovalent co-ions (anions) are shown for the RPM and solvent dielectric saturation model. The ion polarization parameter δ_{2+} is set to -7.5 and also -24 (the last value corresponds to an experimental estimation for the Mg^{2+} ion[58]). The constant δ_{-} is taken as -7.5. Corresponding electrostatic potentials are shown in Figure 4. Notable errors in PB calculations due to the interionic correlations[17,20−23,39,41] are known for highly charged double layers of RPM multivalent electrolytes. From a comparison shown in Figures 3 and 4, one can see that errors due to neglecting solvent saturation and ion polarization effects may be even higher in the case of multivalent counterions. Divalent ions are affected by the polarization charges appearing in nonuniform dielectric and by the polarization of ion hydration shells (the U^{pol} term of the PMF) so much that the magnitude of the electrostatic potential on the ion-accessible surface ($r_0 = 11$ Å) is three times as higher as the magnitude of the MPB potential obtained for the RPM. It is seen from Figure 5 that the dielectric saturation zone in the vicinity of the polyion has a thickness of more than 10 Å at $\delta_{2+} = -24$.

Contributions of the PMF terms $\beta^{-1}\ln \xi(r)$, $e\psi(r)$, $U^{pol}{}_{\nu}(r)$, and $U^{csi}{}_{\nu}(r)$ from eq 16 are shown in Figure 6 (2:1 electrolyte, $\delta_{2+} = -24$). The first, volume exclusion term is negligible. For RPM 2:1 electrolyte, the $U^{csi}{}_{2+}(r)$ term corresponds to a strong attraction of counterions (cations) in addition to the mean electric force, whereas the absolute magnitude of $U^{csi}{}_{-}(r)$ is much lower. It explains the effect of overneutralization obtained for the RPM double layers.[17,22,23,29,41] The picture is different when adding the ionic polarization and solvent dielectric saturation effects. Although the $U^{csi}{}_{2+}(r)$ term is an attractive potential at long distances from the ion-accessible surface, it corresponds to a repulsive force near the cylinder. One can see that there is also a very strong repulsion of divalent ions due to the $U^{pol}{}_{2+}$ term close to the surface of the polyion (the $U^{pol}{}_{2+}$ term is up to $+6kT$ of the magnitude). In the case of 1:1 electrolyte the U^{pol} term is much lower ($<1.5kT$).

The sensitivity of results to parameters of the model has been studied. A replacement of the dielectric cavity diameter $2a_{\epsilon} =$ 6 Å by a value of 4 Å does not affect results obtained for the RPM as predicted by the theory (numerical solution errors result in a difference of corresponding potentials within 1%). Such a comparison made for 1:1 and 2:1 polarizable ions together with dielectric saturation of the solvent shows a sensitivity of the $\psi(r)$ and $\epsilon(r)$ functions to this parameter (Figures 4 and 5). In contrast, curves are not affected by the choice of the internal permittivity ϵ_i of the ion dielectric cavity (a value of 10 instead of 2 was used for comparison, data not shown). It means that this unknown parameter may be set arbitrarily and not considered as a fitting parameter of the model. This result is apparent from the Born formula of the ion solvation energy where the electrostatic energy of an ion depends entirely on the diameter of the cavity. The dielectric constant ϵ_m inside the cylinder does not affect $\psi(r)$, $\epsilon(r)$ and terms of the PMF. The corresponding differences were within several persent when $\epsilon_m = 70$ was used instead of $\epsilon_m = 2$ (data not shown). It confirms earlier results for the RPM[39,41] that the choice of ϵ_m weakly affects the mean electrostatic potential around the highly charged molecule of DNA. The origin of the significant sensitivity of the potential and ionic distributions to the parameter δ_{2+} (Figures 3 and 4) is the dependence $\epsilon(r)$ (eq 7). It is clearly seen when calculations are done with the U^{pol} term but at the solvent uniform dielectric constant. In this case curves are close to those obtained for the RPM (data not shown). The explanation of results shown in Figures 3 and 4 is as follows. The decrease of $\epsilon(r)$ due to dielectric saturation[46,45] causes an additional increase of the energy of an ion. This increase is not itself too high: the simplest estimation based on the Debye−Huckel approximation leads to the energy difference from $+1$ to $+2$ kT for a divalent ion if the solvent permittivity drops from 78 to 50 (Figure 5). But this (together with the additional repulsion of ions due to the U^{pol} term) causes a decrease of the concentration of ions in the dielectric saturation zone. The last decreases the interionic correlations attractive force acting on the counterion, decreases screening of the mean electrostatic field, and increases intensity of the field in this region. The higher electric field leads to stronger additional repulsion of ions from the polyion due to the U^{pol} term in eq 16. Despite the higher attractive mean electric force acting on ions, the resulting balance in forces leads to a lower counterion concentration near the polyion than that for the RPM (Figures 3 and 6). This repulsion of ions must be finally stabilized because the electrostatic field intensity tends to a limiting value at the removal of ions from the polyion.

Looking at Figures 1−5, it is possible to discuss the assumptions used to derive the MPB eqs 4−8 (section Theory). The uniform density solvent model (eqs 1 and 7) would be apparently justified if the dielectric saturation zone around the polyion extended many molecular diameters into the solution. Actually it is not so: this zone involves only a few layers of water molecules (ref 45, Figure 5). In fact this assumption can only be verified by MD simulations and/or experimental data. As follows from recent MD simulations for DNA with ions,[45] no oscillatory behavior of the mean permittivity is observed. For the all-atom model of DNA, the MD simulated dependence $\epsilon(r)$ looks quite similar to curves shown in Figure 5 as well as to a sigmoidal function found in ref 46, where eqs 1−3 are combined with the PB equation. The last may be regarded as a justification of the model. The stability of the ion hydration shells in the electric field of DNA can be verified by a simple estimation. The electrostatic field is order of about 10^8 volts per cm near the ion[64] (i.e. within the first coordination shell of water molecules). This value is notably higher than the obtained upper limit for the mean electrostatic field in the vicinity of the polyion (2×10^6 volts per cm, Figure 4). One may expect that

the solvent shells are not totally destroyed by the field which is much lower than the central field of the ion, although they can be notably affected by this field and by geometry restrictions close to the surface of the macromolecule. But even if the ion hydration shells are partly destroyed, which leads to a lower absolute value of the empirical parameter δ_{2+}, the influence of the polarization forces remains significant in the case of divalent counterions. The last follows from results obtained at $\delta_{2+} = -7.5$ (Figures 3 and 4).

Higher polarization forces at $\delta_{2+} = -24$ cause instability in the main iterative process (9)−(6)−(5)−(4)−(9) and its convergence cannot be obtained. To solve the MPB equations in this case, each change of the dielectric function $\epsilon(r)$ calculated via eq 7 is multiplied by a reducing coefficient τ ranging from 0.3 to 0.5: $\epsilon^{(i+1)} = \epsilon^{(i)} + (\epsilon^{(i+1)} - \epsilon^{(i)})\cdot\tau$. Such a procedure was also applied to calculations at $\delta_{2+} = -7.5$ and for 1:1 salt where the convergence was obtained without reducing changes of ϵ. Comparisons have shown the stability of calculated potentials and ionic distributions in the case of low-polarizable divalent and monovalent counterions irrespective of this reduction. For the model of highly polarizable divalent counterions, the convergence of the main cycle (9)−(6)−(4)−(9) is slow. The stability of the potential and $\epsilon(r)$ function is reached at $\tau = 0.3$ after 14−16 iterations.

Equations 4−8 have been also used to evaluate an influence of dielectric saturation on the free energy of a macromolecule in a solution of electrolyte. The model of a 15 Å radius spherical macroion was explored. All parameters of the solvent and ions are described above. Counterions are divalent. The internal permittivity of the macroion is set to 10; the thickness of the Stern layer is 3 Å. Calculations were performed according to eqs 12−14 with five charging states in the charging integral (13). The model of low-polarizable divalent counerions is applied ($\delta_{2-} = -7.5$). Results are compared with MPB and PB calculations for the uniform permittivity solvent model with equal and different dielectric constants of the solvent and macroion. As follows from results obtained at macroion's charge $Q = +7e$, all the dielectric saturation and ionic polarization effects may be neglected for not-too-highly charged macromolecules, although the dielectric boundary notably affects the long-range electrostatics part of the free energy.[40] Free energy differences at the transfer of a highly charged macroion ($Q = +27e$) from pure water into 1:2 electrolyte solutions are shown in Figure 7 as functions of the ionic strength. One can see that the influence of the dielectric saturation can be notable in the case of a highly charged macromolecule.

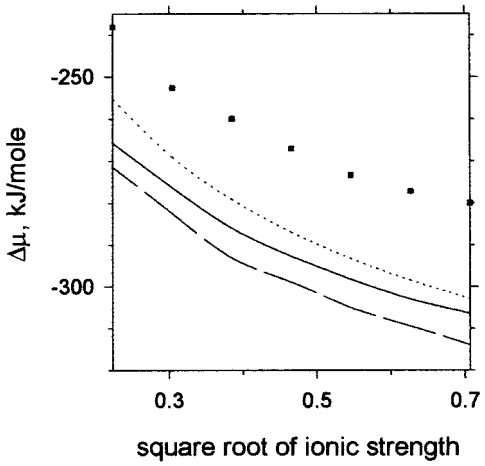

Figure 7. Free energy change $\Delta\mu$ of a 15 Å radius, +27e charge spherical macroion at the transfer of the macroion from pure water into a 1:2 electrolyte solution as a function of ionic strength. The solid and dashed lines are MPB results for the RPM model of electrolyte ($d = 4.0$ Å; the Stern layer thickness is 3 Å; the solvent dielectric constant is 78.5) at dielectric constants of the macroion taken as 10 and 78.5, respectively. The dotted line is $\Delta\mu$ for solutions of the PB equation. The filled squares are MPB results for the solvent dielectric saturation model.

Conclusions

As follows from the present study, the dielectric saturation effects may be neglected in the case of not-too-highly charged macromolecules and monovalent electrolytes. It justifies numerous applications of the PB equation to calculation of the ionization energy of charged groups of proteins. In contrast, neglecting these effects in the case of DNA may lead to errors in potentials. For multivalent electrolytes, not only interionic correlations, but also dielectric saturation and ionic polarization effects should be incorporated into the continuum solvent model.

The present model is a very crude attempt at treating solvent polarization forces acting on ions. The Booth's theory of dielectric saturation is based on some assumptions regarding water structure. The theory was confirmed by experimental results only at electric fields up to 2.5×10^5 volts per cm,[65] whereas fields in the vicinity of the cylindrical approximate model of DNA reach 2×10^6 volts per cm. The use of experimental constants δ_{Na^+} and $\delta_{Mg^{2+}}$ obtained for bulk electrolyte may also be incorrect in the vicinity of the DNA macromolecule. These parameters reflect low polarizability of the ion together with the cluster of frozen water molecules in comparison with an equal volume of pure water.[46] Such a cluster should be affected by the high external electric field of the polyelectrolyte charges, especially for multivalent ions since their clusters contain two coordination shells of water molecules.[57,58] Nevertheless, one can see from Figure 4 that a replacement of $\delta_{Mg^{2+}} = -24$ by $\delta_{Mg^{2+}} = -7.5$ also leads to a significant repulsion of divalent counterions from DNA and a notable discrepancy in potentials calculated for the RPM and for the solvent dielectric saturation model.

It is important to note that for multivalent electrolytes the true electrostatic potentials around DNA have never been obtained by experiments or MD simulations. An experimentally measured potential was obtained for DNA in a monovalent electrolyte diluted solution at 14 Å distance from the helical axis.[66] This measurement has verified the PB calculations, but it does not allow us to draw conclusions because for a 1:1 electrolyte the PB, RPM MPB, and the present MPB calculations result in almost identical potentials at $r = 14$ Å (Figure 2). A reported measurement of divalent counterion (Ba^{2+}) distributions around DNA fragments in a very diluted $BaCl_2$ solution[67] does not allow us to draw a conclusion either. An analysis of Figures 2 and 3 of that work shows that experimental curves I(Q) at larger Bragg wavenumber Q are sensitive to the ionic distributions near the polyion. Looking at Figure 3 of the present work, one can see that the divalent counterion distribution obtained for the MPB eqs 4−9 at $\delta_{2+} = -7.5$ is notably deviated from the PB distribution at less than 10 Å separation from the polyion surface. But at such distances, effects of the 3D structure of a real macromolecule may not be ignored to calculate the ionic distributions near the macromolecule. As a result, it is impossible to separate the dielectric saturation and 3D all-atom structure effects as well as to see the true ionic distributions near DNA from this experiment. Unfortunately, numerous measurements of binding to polyelectrolytes of multivalent ions and oligocationic ligands do not reveal the true picture since those data were obtained for dilute multivalent ion (ligand) solutions at

low to moderate concentration of univalent salt. In this case the mean electrostatic field is unperturbed by the presence of multivalent ions and the electrostatic potential is governed by monovalent ions.[68] As follows from the present work, the PB equation is a reasonable approximation for electrostatics of DNA in 1:1 electrolyte solutions, so the observed agreement with PB results can be explained. In contrast, explanation of conformational transitions and polyelectrolyte associations in multivalent solutions meets difficulties. For example, it is known that both the collapse of DNA to a highly compact form and the intermolecular condensation of DNA to an ordered phase can be induced by the addition of multivalent ions.[69] The explanation of direct measurements of repulsive force between polyelectrolyte molecules in multivalent ion solutions[70,71] remains to be questionable. An attractive contribution to the interaction was explained by the correlation between the ion clouds of different DNA polyions[72] or by introduction of the long-range hydration forces.[73] Thus, there is no evidence that electrical double-layer theories have been experimentally verified for multivalent ion solutions.

The final conclusion is that even for diluted solutions of multivalent ions, water dielectric saturation and ionic polarizability may have impact on the thermodynamics of highly charged polyions and properties of the polyelectrolyte solution. In addition to the size of ions, two new adjustable parameters appear in the continuum solvent model: the radius of the dielectric cavity of an ion and the dependence of the solvent permittivity on the electric field and ionic concentrations. The applicability of eqs 1 and 7 has never been proved at magnitudes of the electric field corresponding to fields in the vicinity of the DNA macromolecule. A verification of the theory by experiments or MD simulations would clarify this question.

Appendix 1: Free Energy of Uncharged Macromolecule in Electrolyte Solution

A change of the electrostatic part of the Helmholtz free energy at a transfer of an uncharged molecule into the volume V of electrolyte, containing N ions, is the change of the chemical potential of all the ions of the system. The chemical potential of an ion is independent of the coordinates of the ion, but it undergoes a change after placing the macromolecule into electrolyte. At a long distance from the molecule, the chemical potential of an ion of species ν can be written as

$$\mu_\nu^{(i)} = \beta^{-1} \ln n_\nu^{(i)} - \frac{e^2 Z_\nu^2}{2\epsilon_0} \frac{K^{(i)}}{1 + K^{(i)} d} + \mu_\nu^0(T)$$

where $i = 1, 2$; $n_\nu^{(1)}$ and $n_\nu^{(2)}$ are ion concentrations of the ionic species ν at infinity before and after the transfer of the molecule, respectively; $K^{(1)}$ and $K^{(2)}$ are the corresponding Debye−Huckel lengths for bulk electrolyte; Z_ν is the valency of the ion; $\beta = 1/kT$, $K^{(i)} = \sqrt{(4\pi\beta e^2/\epsilon_0)\sum Z_\nu^2 n_\nu^{(i)}}$; ϵ_0 is the dielectric constant of bulk water. The term $-(e^2 Z_\nu^2/2\epsilon_0)(K/(1 + Kd))$ is the Debye−Huckel energy of a spherical ion in bulk electrolyte, d is the diameter of the ion. The change of the free energy of all the ions is

$$W_0 = \Delta F_{\text{ions}} = \sum_\nu N_\nu \beta^{-1} \ln \frac{n_\nu^{(2)}}{n_\nu^{(1)}} - \sum_\nu N_\nu \frac{e^2 Z_\nu^2}{2\epsilon_0} \left(\frac{K^{(2)}}{1+K^{(2)}d} - \frac{K^{(1)}}{1+K^{(1)}d} \right) \quad (1A)$$

The definition of $n_\nu^{(2)}$ is

$$n_\nu^{(2)} \int_V g_\nu(\mathbf{r}) \mathrm{d}^3\mathbf{r} = N_\nu = n_\nu^{(1)} V$$

where $g_\nu(\mathbf{r})$ is the distribution function of the ionic species ν and N_ν is a total number of ions of species ν. It follows from the last expression that

$$\frac{n_\nu^{(2)}}{n_\nu^{(1)}} = \frac{V}{\int_V g_\nu(\mathbf{r}) \mathrm{d}^3\mathbf{r}} = \frac{V}{V - \int_V (1 - g_\nu(\mathbf{r})) \mathrm{d}^3\mathbf{r}} \approx 1 + \frac{1}{V} \int_V (1 - g_\nu(\mathbf{r})) \mathrm{d}^3\mathbf{r} \quad (2A)$$

Similarly, one can derive

$$\frac{K^{(2)}}{K^{(1)}} = \sqrt{\frac{\sum Z_\nu^2 n_\nu^{(2)}}{\sum Z_\nu^2 n_\nu^{(1)}}} \approx 1 + \frac{1}{2}\delta \text{ and } \frac{1+K^{(2)}}{1+K^{(1)}} \approx 1 + \frac{1}{2} \frac{K^{(1)} d}{1+K^{(1)}d} \delta$$

where

$$\delta = \frac{1}{V} \frac{\sum Z_\nu^2 n_\nu^{(1)} \int (1 - g_\nu(\mathbf{r})) \mathrm{d}^3\mathbf{r}}{\sum Z_\nu^2 n_\nu^{(1)}}$$

and, taking into account that $\delta \ll 1$, one has

$$\frac{K^{(2)}/K^{(1)}}{(1 + K^{(2)}d)/(1 + K^{(1)}d)} \approx 1 + \frac{1}{2}\delta \frac{1}{1 + K^{(1)}d} + O(\delta^2) \quad (3A)$$

Finally, after substitution of eqs 2A and 3A into eq 1A and rearrangement, one obtains eq 14 for W_0 which is work against the partial pressure of ionic gas during the transfer of the uncharged macromolecule into electrolyte. The term $-Z_\nu^2 e^2 K/(4\epsilon_0(1+Kd)^2)$ comes from nonideality of ionic gas and reflects its higher compressibility due to the Coulombic interactions of ions.

References and Notes

(1) Young, M. A.; Jayaram, B.; Beveridge, D. L. *J. Am. Chem. Soc.* **1997**, *119*, 59.
(2) Cheatham, T. E., III; Kollman, P. A. *J. Mol. Biol.* **1996**, *259*, 434.
(3) Yang, L.; Pettitt, B. M. *J. Phys. Chem.* **1996**, *100*, 2564.
(4) Young, M. A.; Ravishanker, G.; Beveridge, D. L. *Biophys. J.* **1997**, *73*, 2313.
(5) Sprous, D.; Young, M. A.; Beveridge, D. L. *J. Phys. Chem. B* **1998**, *102*, 4658.
(6) Lamm, G.; Wong, L.; Pack, G. R. *Biopolymers.* **1994**, *34*, 227.
(7) Jayaram, B.; DiCapua, F.; Beveridge, D. *J. Am. Chem. Soc.* **1991**, *113*, 5211.
(8) Jayaram, B.; Sharp, K. A.; Honig, B. *Biopolymers* **1989**, *28*, 975.
(9) Luty, B. A.; Davis, M. E.; McCammon, J. A. *J. Comput.Chem.* **1992**, *13*, 1114.
(10) Bashford, D.; Karplus, M. *Biochemistry* **1990**, *29*, 10219.
(11) Bashford, D.; Karplus, M. *J. Phys. Chem.* **1991**, *95*, 9556.
(12) Takahashi, T.; Nakamura, H.; Wada, A. *Biopolymers* **1992**, *32*, 897.
(13) Oberoi, H.; Allewell, N. M. *Biophys. J.* **1993**, *65*, 48.
(14) Loewenthal, R.; Sancho, J.; Reinikainen, T.; Fersht, A. R. *J. Mol. Biol.* **1993**, *232*, 574.
(15) Antosiewicz, J.; McCammon, J. A.; Gilson, M. K. *J. Mol. Biol.* **1994**, *238*, 415.
(16) Schaefer, M.; Sommer, M.; Karplus, M. *J. Phys. Chem. B* **1997**, *101*, 1663.
(17) Carnie, S. L.; Torrie, G. M. *Adv. Chem. Phys.* **1984**, *56*, 141.
(18) Murthy, C. S.; Bacquet, R. J.; Rossky, P. J. *J. Phys. Chem.* **1985**, *89*, 701.
(19) Mills, P.; Anderson, C. F.; Record, M. T., Jr. *J. Phys. Chem.* **1985**, *89*, 3984.
(20) Degreve, L.; Lozada-Cassou, M. *Mol. Phys.* **1995**, *86*, 759.

(21) Das, T.; Bratko, D.; Bhuiyan, L. B.; Outhwaite, C. W. *J. Phys. Chem.* **1995**, *99*, 410.
(22) Das, T.; Bratko, D.; Bhuiyan, L. B.; Outhwaite, C. W. *J. Chem. Phys.* **1997**, *107*, 9197.
(23) Montoro, J. C. G.; Abascal, J. L. F. *J. Chem. Phys.* **1995**, *103*, 8273.
(24) Arakawa, T.; Timasheff, S. N. *Methods Enzymol.* **1985**, *114*, 49.
(25) Bacquet, R. J.; Rossky, P. J. *J. Phys. Chem.* **1984**, *88*, 2660.
(26) Gonzales-Tovar, E.; Lozada-Cassou, M.; Henderson, D. *J. Chem. Phys.* **1985**, *83*, 361.
(27) Kjellander, R.; Marcelja, S. *J. Chem. Phys.* **1985**, *82*, 2122.
(28) Klement, R.; Soumpasis, D. M.; Jovin, T. M. *Proc. Natl. Acad. Sci. U.S.A.* **1991**, *88*, 4631.
(29) Levine, S.; Bell, G. M. *J. Phys. Chem.* **1960**, *64*, 1188.
(30) Levine, S.; Bell, G. M. *Discuss. Faraday Soc.* **1966**, *42*, 69.
(31) Bell, G. M.; Levine, S. in *Chemical Physics of Ionic Solutions*; Conway, B. E., Barradas, R. G., Eds.; Wiley: New York, 1966.
(32) Levine, S.; Outhwaite, C. W. *J. Chem. Soc., Faraday Trans. 2* **1978**, *74*, 1670.
(33) Outhwaite, C. W.; Bhuiyan, L. B. *Mol. Phys.* **1991**, *74*, 367.
(34) Outhwaite, C. W.; Bhuiyan, L. B. *J. Chem. Soc., Faraday Trans. 2* **1983**, *79*, 707.
(35) Outhwaite, C. W. *J. Chem. Soc., Faraday Trans. 2* **1978**, *74*, 1214.
(36) Outhwaite, C. W. *Mol. Phys.* **1974**, *27*, 561.
(37) Outhwaite, C. W. *Mol. Phys.* **1976**, *31*, 1345.
(38) Outhwaite, C. W. *Mol. Phys.* **1983**, *48*, 599.
(39) Gavryushov. S.; Zielenkiewicz, P. *J. Phys. Chem. B* **1997**, *101*, 792.
(40) Gavryushov. S.; Zielenkiewicz, P. *J. Phys. Chem. B* **1997**, *101*, 10903; Errata: **1998**, *102*, 8640.
(41) Gavryushov. S.; Zielenkiewicz, P. *Biophys. J.* **1998**, *75*, 2732.
(42) Jin, R.; Breslauer, K. *J. Proc. Natl. Acad. Sci. U.S.A.* **1988**, *85*, 8939.
(43) Barawkar, D. A.; Ganesh, K. N. *Nucleic Acids Res.* **1995**, *23*, 159.
(44) Yang, L.; Weerasinghe, S.; Smith, P. E.; Pettitt, B. M. *Biophys. J.* **1995**, *69*, 1519.
(45) Young, M. A.; Jayaram, B.; Beveridge, D. L. *J. Phys. Chem. B* **1998**, *102*, 7666.
(46) Lamm, G.; Pack, G. R. *J. Phys. Chem. B* **1997**, *101*, 959.
(47) Booth, F. *J. Chem. Phys.* **1951**, *19*, 391, 1327, 1615.
(48) Rashin, A. A.; Honig, B. *J. Phys. Chem.* **1985**, *89*, 5588.
(49) Nina, M.; Beglov, D.; Roux, B. *J. Phys. Chem. B* **1997**, *101*, 5239.
(50) Luo, R.; Moult, J.; Gilson, M. K. *J. Phys. Chem. B* **1997**, *101*, 11226.
(51) Chan, D. Y. C.; Mitchell, D. J.; Ninham, B. W. *J. Chem. Phys.* **1979**, *70*, 2946.
(52) Roux, B.; Yu, H.-A.; Karplus, M. *J. Phys. Chem.* **1990**, *94*, 4683.
(53) Jayaram, B.; Fine, R.; Sharp, K.; Honig, B. *J. Phys. Chem.* **1989**, *93*, 4320.
(54) Hummer, G.; Pratt, L. R.; Garcia, A. E. *J. Phys. Chem.* **1996**, *100*, 1206.
(55) Hyun, J.-K.; Ichiye, T. *J. Phys. Chem. B* **1997**, *101*, 3596.
(56) Landau, L. D.; Lifshitz, E. M. *Electrodynamics of continuous media*; Pergamon Press: Oxford, 1960.
(57) Haggis, G. H.; Hasted, J. B.; Buchanan, T. J. *J. Chem. Phys.* **1952**, *20*, 1452.
(58) Hasted, J. B.; Ritson, D. M.; Collie, C. H. *J. Chem. Phys.* **1948**, *16*, 1.
(59) Prigogine, I.; Mazur, P.; Defay, R. *J. Chim. Phys.* **1953**, *50*, 146.
(60) Bolt, G. H. *J. Colloid Sci.* **1955**, *10*, 206.
(61) Sparnaay, M. J. *Rec. Trav. Chim. Pays-Bas* **1958**, *77*, 872.
(62) Eagland, D. In *Water. A comprehensive treatise*; Franks, F., Eds.; Plenum Press: Oxford, 1975; Vol. 5.
(63) Gilson, M. K.; Sharp, K. A.; Honig, B. H. *J. Comput. Chem.* **1988**, *9*, 327.
(64) Conway, B. E. *Ionic Hydration in Chemistry and Biophysics*; Elsevier: New York, 1981.
(65) Malsch, J. *Phy. Z.* **1928**, *29*, 770.
(66) Hecht, J. L.; Honig, B.; Shin, Y.-K.; Hubbel, W. L. *J. Phys. Chem.* **1995**, *99*, 7782.
(67) Chang, S.-L.; Chen, S.-H.; Rill, R. L.; Lin, J. S. *J. Phys. Chem.* **1990**, *94*, 8025.
(68) Stigter, D.; Dill, K. A. *Biophys. J.* **1996**, *71*, 2064.
(69) Record, M. T., Jr.; Mazur, S. J.; Melancon, P.; Roe, J.-H.; Shaner, S. L.; Unger, L. *Annu. Rev. Biochem.* **1981**, *50*, 997.
(70) Rau, D. C.; Lee, B.; Parsegian, V. A. . *Proc. Natl. Acad. Sci. U.S.A.* **1984**, *81*, 2621.
(71) Rau, D. C.; Parsegian, V. A. *Biophys. J.* **1992**, *61*, 246.
(72) Guldbrand, L.; Nilsson, L. G.; Nordenskiold, L. *J. Chem. Phys.* **1986**, *85*, 6686.
(73) Gruen, D. W. R.; Marcelja, S. *J. Chem. Soc., Faraday Trans. 2* **1983**, *79*, 225.